Available online at www.sciencedirect.com
SCIENCE DIRECT®
Catalysis Today 101 (2005) 155–162
CATALYSIS TODAY
www.elsevier.com/locate/cattod

Quantum chemical modelling of the process of lithium insertion into WO_3 films

E. Broclawik [a,*], A. Góra [a], P. Liguzinski [b], P. Petelenz [b], M. Slawik [b]

[a] *Institute of Catalysis and Surface Chemistry, Polish Academy of Sciences, ul. Niezapomianjek 8, Cracow 30239, Poland*
[b] *K.Gumiński Department of Theoretical Chemistry, Jagiellonian University, Cracow, Poland*

Available online 7 March 2005

Abstract

Lithium intercalation into tungsten oxide, which is the crucial process utilized in electrochromic devices, is studied by quantum chemistry methods. The oxide phase is represented by a series of model clusters with the dangling bonds saturated by hydrogen atoms. The calculations, with full geometry optimisation, are performed using the DFT approach within the LDA approximation. Based on the results, suitable clusters are selected for studying lithium penetration into the oxide structure. Lithium stabilisation energy and energy barriers for transport in the oxide phase are calculated for the conditions simulating insertion of the lithium cation into electrically neutral oxide, intercalation induced electrochemically by electron injection from the cathode, and lithium elimination from the oxide at reversed voltage bias. The results are discussed in the context of recent calculations by other authors of lithium stabilisation energy in the polymer electrolyte, used as the other component of an electrochromic device. It is hoped that a combination of both approaches will allow in the future to model lithium balance between the oxide and the polymer phase.

Keywords: Electrochromic colouration; Li intercalation; Tungsta smart windows; TDDFT modelling

1. Introduction

Technological importance of transition metal oxides is widely recognised, and commonly associated with their role as heterogeneous catalysts. Yet, there are also other important areas of their actual or potential usefulness, such as, e.g. energy management, smart windows, displays, etc. This group of applications is based on the ability of some oxides to change colour as a consequence of electrochemical processes. For instance, thin layers of tungsten oxide are known to change from colourless to dark blue when exposed to electron injection from the cathode, accompanied by cation insertion from the anode. In typical conditions the cations are those of lithium, and an aqueous solution or a polymer electrolyte serves as their reservoir. The colour sets in gradually, at a rate commensurate with that of lithium migration into the oxide. When the electric field is switched off, the colouration persists, with a slight tendency to slow bleaching. The blue colour can be totally removed by an analogous electrochemical process at reversed electrode bias.

Apart from their technological consequences, the above phenomena are interesting in their own right. There is extensive experimental literature concerning the conditions and mechanism of the electrochemical processes involved [1–7]. Surprisingly enough, theoretical papers are relatively scarce, and address mostly the assignment of the electronic transition that gives rise to the observed colouration. There are essentially two alternative explanations. According to one, optical absorption is due to the valence-to-conduction-band transition [1,8], whereas the other interpretation attributes the colour to photon-induced polaron hops between the tungsten ions in different valence states [4,9–13]. Accordingly, theoretical effort has been focused either on the calculations of the tungsten oxide band structure [11,14] or on semiphenomenological models describing polaron hopping and related optical absorption [1,4,9,10].

On the other hand, the microscopic picture of electrochemical insertion of the lithium ion into the oxide lattice is sorely needed to improve the understanding of lithium

* Corresponding author. Tel.: +48 126336377; fax: +48 126340515.
E-mail address: broclawi@chemia.uj.edu.pl (E. Broclawik).

0920-5861/$ – see front matter © 2005 Elsevier B.V. All rights reserved.
doi:10.1016/j.cattod.2005.01.013

balance between the oxide phase and the polymer electrolyte used in electrochromic devices, but seems to have escaped the attention of the theorists. Apart from purely phenomenological analyses [15,16], the recent paper [17] dealing with lithium penetration into vanadium oxide, treated by molecular dynamic simulations, is a laudable exception. By and large, it seems that the standard quantum chemical methodology is completely absent from this field, while it was applied with considerable success to describe other properties of metal oxide systems [18–26]. A combination of the DFT method capable of handling the heavy transition metal atoms without investing prohibitive computational effort, with cluster models, especially appropriate for the thin, largely amorphous layers of the oxide material, seem to be the approach of choice for the description of electrochromic phenomena. The present paper is an attempt to build and test the main premises of such a model description, proposed in the hope that in a long run it may provide new insights into the field.

2. Quantum chemical modelling protocol

In the present paper, tungsten oxide is represented by a series of model clusters of varying size and topology, dependent on the specific question to be addressed. In all cases hydrogen atoms artificially saturate the dangling oxygen bonds at cluster boundaries. This saturation scheme guarantees that the model clusters are electrically neutral (unless charge injection from the electrode is simulated), with assumed formal charges +6 for tungsten, −2 for oxygen and +1 for hydrogen, mimicking the situation in fully oxidised tungsta.

In order to maintain the numerical effort at a reasonable level of practical tractability, the size of the model clusters must inevitably be small. At the same time, it must be large enough to capture the physically relevant features of the real system. This results in a compromise, determined by the kind of phenomena to be simulated and by the requirements of the quantum chemical methods to be used.

Based on our earlier experience with other transition metal oxides [24–26], the DFT methodology was found to give the best prospects for reaching the conclusions at minimum cost; the actual calculations were carried out by means of the Dmol software included in the package of Molecular Simulations© [27]. The local spin density approximation (VWN potential) in the DNP basis set was chosen for further use. Atomic charges were evaluated according to the Hirshfeld partitioning scheme, widely accepted as the most reliable in the case of numerical DFT calculations. Molecular structures were drawn with the Weblab Viewer program (Copyright© 2000 by MSI).

2.1. Tests of the model approach

Preliminary calculations performed for a series of clusters mimicking the structure of solid WO_3 have shown that the clusters built of four and nine octahedral units ($W_4O_{20}H_{16}$ and $W_9O_{42}H_{30}$, respectively) reasonably represent the surface layer of the oxide. Subsequently, the effect of inter-layer interactions was studied on the double-layer $W_8O_{36}H_{24}$ cluster, and the triple-layer $W_{12}O_{52}H_{36}$ cluster was introduced to investigate the differences between the surface layer and the bulk of the oxide. The calculations entailed full geometry optimisation and produced geometric parameters in reasonably good agreement with crystallographic data (vide infra).

According to the literature, the lengths of the diverse W–O bonds in WO_3 structures range between 1.80 and 2.01 Å [2]. Owing to their small size and idealized boundaries (dangling bonds saturated by hydrogen atoms instead of the surrounding framework), the cluster models practically accessible to quantum chemical calculations are inherently incapable of reproducing the bond diversity actually encountered in the solid WO_3. For this reason as the reference parameter representing globally the experimental data we have chosen the average of the bond lengths equal to 1.92 Å. The mean W–O bond distance calculated for the inner part of the studied clusters (corresponding to crystal bulk) was equal to 1.92 Å for the $W_4O_{20}H_{16}$ cluster and 1.93 Å for the larger ones ($W_8O_{36}H_{24}$ and $W_9O_{42}H_{30}$). These numbers compare very well with the crystallographic average value of 1.92 Å, supporting our initial conjecture that the selected models should describe the geometry of the WO_3 structure sufficiently well. In addition, the bond lengths calculated for the outer W–O bonds (in the W–O–H units terminating the cluster), falling in the range between 1.93 and 1.99 Å, show that hydrogen atoms may be used to terminate the cluster without introducing major distortion of the system.

For the two-layer $W_8O_{36}H_{24}$ cluster we have also attempted to examine the main features of the electronic structure by comparing it to the bulk electronic structure calculated for cubic WO_3 and $LiWO_3$ systems by first-principles band structure theory with similar numerical parameters [1]. Figs. 1 and 2 show the graphs of eigenvalue distribution calculated for the $W_8O_{36}H_{24}$ cluster and for the

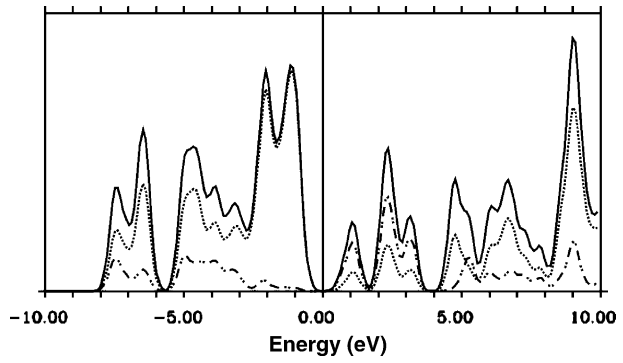

Fig. 1. Eigenvalue distribution for the $W_8O_{36}H_{24}$ cluster (zero on the abscissa axis corresponds to the Fermi level, ordinate axis: arbitrary units); full line: total distribution, dotted line: oxygen-2p contribution, dash-dot line: tungsten-5d contribution.

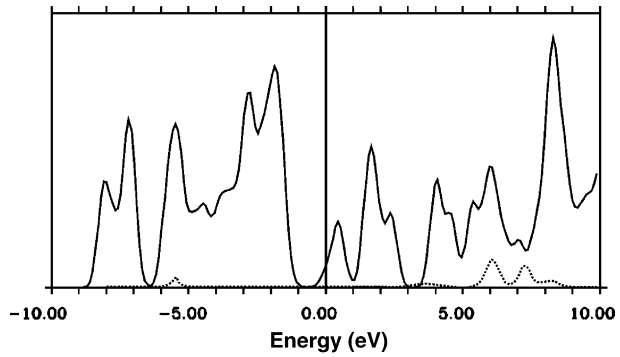

Fig. 2. Eigenvalue distribution for the $LiW_8O_{36}H_{24}$ cluster (*X* and *Y* axes defined as in Fig. 1); full line: total distribution, dotted line: lithium-2s contribution (10×).

same cluster with the lithium atom located in its centre. These graphs may be compared with the density of states (DOS) diagrams that are commonly used to analyse the electronic structure of bulk materials [1]. It is very understandable that the results obtained for a cluster of finite size cannot fully reproduce the density of states for bulk oxide. In addition, the LDA approximation is known to systematically underestimate the band gap and therefore only qualitative features of the electronic structure may be discussed here. Nevertheless, the general shape of the electron distribution is reasonably reproduced (especially in view of the inherent differences between the applied approaches); in addition, some details of the bulk electronic structure have clear counterparts in our calculations. The Fermi level positioned within the forbidden energy gap is consistent with the wide-gap semiconducting character of the oxide, experimentally characterized as a semiconductor with an indirect transition across the band gap of roughly 3.25 eV [1]. Our calculated estimate of the gap is obviously underestimated, however, it is close to the value calculated by Granqvist (0.6 eV [1]). The character of the valence and conduction bands, dominated by the O 2p and W 5d orbitals, respectively, was also to be expected. In the case of the $LiW_8O_{36}H_{24}$ cluster the Fermi level is shifted into the conduction band, while the character of the valence band is very similar to that of the pure oxide. The Li 2s orbital is located around 6 eV above the Fermi level, which implies that lithium essentially remains ionised in the oxide and the transferred electrons occupy the tungsten d orbitals dominating the bottom of the conduction band.

2.2. Modelling of lithium migration

The analysis of the geometric and electronic structure of the model clusters, described in the preceding subsection, encouraged us to use such clusters for simulating the behaviour of lithium ions intercalated into tungsta films. In order to pinpoint the difference between the surface layer and the bulk of the oxide, in addition to those previously described we have now introduced the triple-layer $W_{12}O_{52}H_{36}$ cluster. Along with the double-layer $W_8O_{36}H_{24}$, it is used to study the process of lithium ion penetration into the oxide structure. In the following, these two models will be referred to as W8 and W12, respectively.

As the starting point for the modelling of the composite system we took the appropriate tungsten–oxygen 'cage' (W8 or W12) with the lithium atom positioned in its centre. The geometry of the cluster was then fully optimised; independent optimisation demonstrated that the presence of lithium in the centre barely affects the geometric parameters of the cage.

Subsequently, the energy profile for the process of lithium migration out of the cage was simulated by performing a series of single-point calculations (without geometry re-optimisation) with the lithium shifted out stepwise along the line drawn from the central position and intersecting the centre of the surface layer. Freezing the geometric parameters of the oxide cage in our gas-phase model calculations may seem a severe limitation; nevertheless it partly takes into account the constraints imposed by the surrounding framework. Full geometry relaxation would obviously lower not only the calculated energy barriers but also the energies at the minima, which in view of our final target should strengthen the conclusions concerning the cation stability inside the cage with various charge states. The calculations were performed independently for the double-layer and for the triple-layer cluster, each in two alternative charge states (neutral and +1 charged). The neutral model is physically interpretable either as the lithium positive ion present in the cage into which one electron has already been injected, or as the effect of neutral lithium insertion into the neutral oxide framework. The charged model mimics the interaction of Li^+ with the neutral cage.

In addition, in order to probe the de-intercalation process, the calculations of the energy profile for lithium migration were repeated for the triple-layer (W12) cluster with +2 formal charge on the system.

3. Results

The optimised geometries of the double-layer W8 and triple-layer W12 clusters are shown in the structural parts (lower panel) of Figs. 3 and 4, respectively. The lithium atom is shown schematically at an arbitrarily imposed large distance from the cluster, merely to depict the direction of the reaction co-ordinate describing the process of lithium insertion into the cluster of tungsten oxide. The reaction co-ordinate is set equal to zero for lithium aligned exactly with the surface layer of the cluster; accordingly, the decreasing positive values of the reaction co-ordinate represent the approach of the lithium moiety towards the surface, while the negative values correspond to the interior of the cluster. In this co-ordinate frame the abscissa of the centre is −2 Å for the W8 cluster, and −4 Å for the bigger W12 cluster.

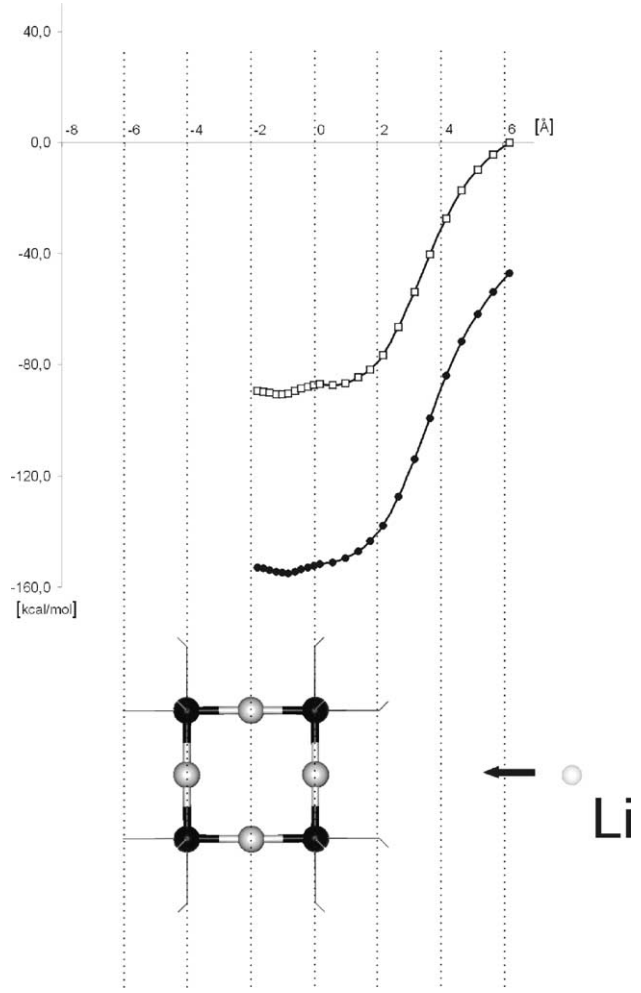

Fig. 3. Lower panel—geometric structure of the $W_8O_{36}H_{24}$ cluster (grey spheres: oxygen atoms, black spheres: tungsten atoms, terminating OH groups shown only schematically). Upper panel—energy profiles for the process of lithium cation penetration into the W8 clusters: $[W_8O_{36}H_{24}]^{-1}$ (black circles) and $[W_8O_{36}H_{24}]^{0}$ (empty squares). Zero on the ordinate axis is at the sum of the total energies of the isolated Li^+ ion and the appropriate lithium-free oxide cage.

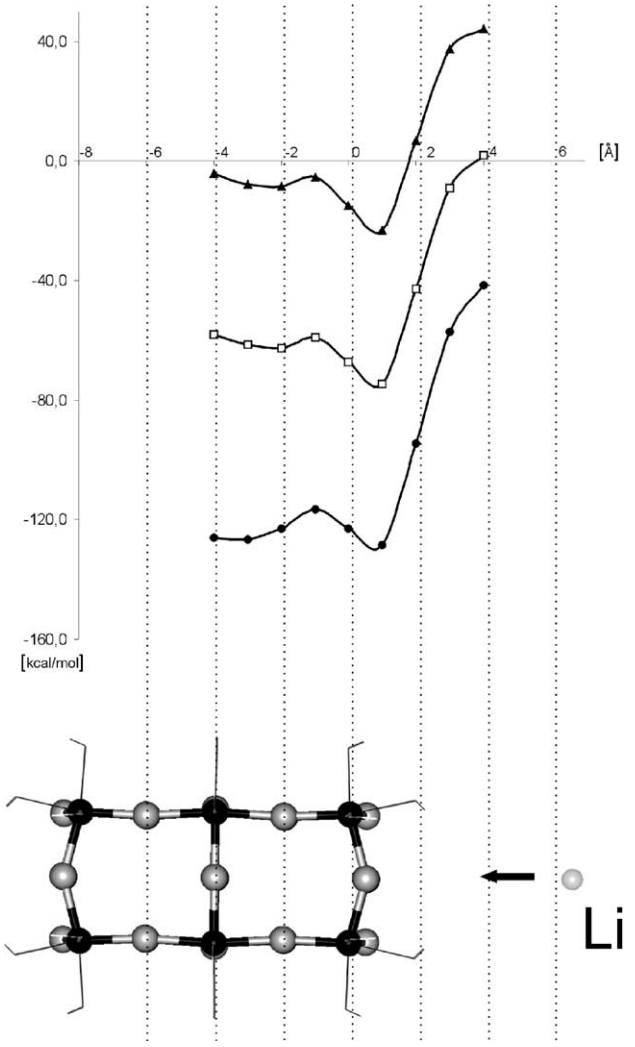

Fig. 4. Lower panel—geometric structure of the $W_{12}O_{52}H_{36}$ cluster. Upper panel—energy profiles for the process of lithium cation penetration into the W12 clusters: $[W_{12}O_{52}H_{36}]^{-1}$ (black circles), $[W_{12}O_{52}H_{36}]^{0}$ (empty squares) and $[W_{12}O_{52}H_{36}]^{+1}$ (black triangles). Zero on the ordinate axis and atom labels defined as in Fig. 3.

It has already been mentioned that the electrically neutral model cluster, consisting of lithium separated by some distance from the oxide cage, might alternatively represent either a system composed of two neutral entities (the oxide and the lithium atom), or the lithium cation and the negatively ionised oxide (with an extra electron injected from the electrode). It was not known a priori which one of the two possibilities would actually be predicted by the calculations. Should the former be the case, the quantum chemical description of the system would fail to account for an essential feature of the experiments that are to be interpreted (where the surrounding electrolyte contains the Li^+ ions), and its interpretational usefulness would be questionable. Therefore, the behaviour of the model in this respect became a crucial test.

The results of the test are shown in Figs. 5 and 6, displaying the dependence of the lithium charge on the reaction co-ordinate. It is readily seen that the charge on lithium approaches +1 for large separation of the subsystems for any model and any charge state. Moreover, the trends in Li charge variation along the reaction co-ordinate coincide perfectly for the different charge states of the cluster (the circles are practically superimposed on the squares) and for the two different models of the oxide (Fig. 5 versus Fig. 6). These two arguments validate the qualitative description of the system as an entity composed of the lithium cation and of the oxide cage, the latter carrying a charge dependent on the experimental conditions (i.e., on charging from the electrode, or its absence), and thereby confirm the applicability of the applied quantum chemical model.

Figs. 5 and 6 also show that the net charge on lithium remains positive (about 0.2) even when the ion is deeply embedded in the oxide. This is not surprising in view of simple energy considerations. In fact, independent calcula-

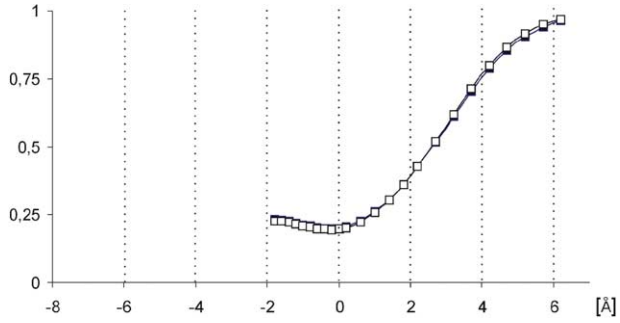

Fig. 5. Dependence of lithium charge on the reaction co-ordinate for the W8 clusters: $[W_8O_{36}H_{24}]^{-1}$ (empty squares) and $[W_8O_{36}H_{24}]^{0}$ (black squares).

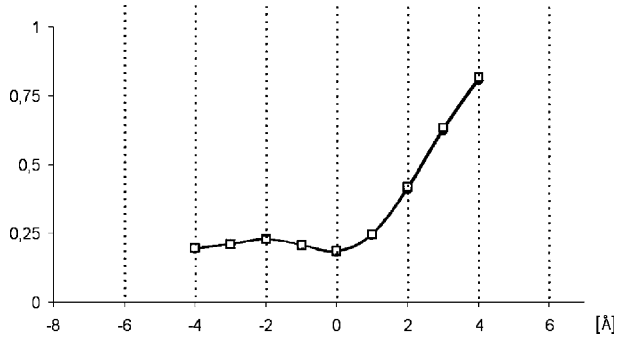

Fig. 6. Dependence of lithium charge on the reaction co-ordinate for the W12 clusters: $[W_{12}O_{52}H_{36}]^{-1}$ (black circles), $[W_{12}O_{52}H_{36}]^{0}$ (empty squares).

tions performed for bare clusters, neutral and charged by one electron, clearly indicate that these systems exhibit a very strong tendency to accept electrons. The electron affinity, roughly estimated from the total energy differences of the corresponding charged and neutral systems, is equal to 3.5 and 4.5 eV for W8 and W12, respectively. Account taken of the substantial electrostatic stabilisation of the cation in a negatively charged lattice, these data, when combined with the low ionisation potential of lithium (estimated from analogous calculations as 5.5 eV), lead to the qualitative conclusion that it is in fact the lithium cation that is transported within the system, in perfect accordance with the commonly accepted intuitive view [3,6,28]. In model calculations performed in this work the effect of additional stabilisation of the lithium cation outside the crystallite by dielectric medium was not incorporated directly, although indisputably it is also important. Thus the asymptotic behaviour of the isolated neutral $Li/W_nO_mH_p$ system could not be quantitatively assessed. Nevertheless, the consistency of the charge on the lithium for different charge states of the cluster lends additional credence to our description of the crystallite interior.

This also allows one to draw the potential energy curves for the various charge states on the common energy scale, by taking the zero of energy as the energy of the two subsystems with separated charges, placed at an infinite distance from each other. In the following, it will be defined as the sum of the (independently calculated) total energies of the separate Li^+ ion and of the appropriate lithium-free oxide cage, i.e. $[W_8O_{36}H_{24}]^{-1}$, $[W_8O_{36}H_{24}]^{0}$, $[W_{12}O_{52}H_{36}]^{-1}$, $[W_{12}O_{52}H_{36}]^{0}$ or $[W_{12}O_{52}H_{36}]^{+1}$; the corresponding composite system could be envisaged as the lithium cation located at an infinite distance from the oxide surface.

The common zero of energy being now established, the energy profiles obtained for different charge states of the cluster may be directly compared; moreover, future inclusion of the electrostatic stabilisation of lithium ions in the surrounding electrolyte solution is greatly facilitated.

The energy profiles for the process of lithium penetration into the W–O clusters are shown in Figs. 3 and 4, exemplified on the W8 and W12 models.

In the case of the W8 model, the results are displayed for two charge states, neutral and +1. In both instances, a very shallow and broad energy minimum is predicted for lithium located inside the cluster, which is intuitively unexpected and may be considered somewhat suspect. This provokes the question whether the W8 model is sufficiently realistic to be trusted. Closer inspection indicates that it does not reflect the situation in the bulk of the crystallite, being in fact constructed from two surface layers, directly connected and interacting. The energy gained by the system on lithium approach to the cage seems to come mostly from the lithium-surface affinity and its variation inside the cluster is marginal, which may suggest that specific local interaction of lithium with the oxide framework is not included. For this reason, the smaller model, tempting as it is on account of its numerical effectiveness has to be abandoned as probably unrealistic.

This conjecture is confirmed by the results obtained for the W12 model, containing in addition a third (inner) layer separating the two ‘surfaces’. Evidently, its presence has dramatic influence on the energy profile: the minimum is now much more pronounced and located out of the crystallite. This corresponds to lithium adsorption and perfectly agrees with intuitive expectations, supporting the validity of the W12 model. Accordingly, from now on this model is earmarked for further use.

The predicted energy profile is now much richer, properly reflecting the specific interaction with the oxide lattice. There are new features: barriers just below the surface and an additional minimum in the interior of the cluster. The barrier is about 16 kcal/mol for the cluster charge of +1, i.e. for Li^+ penetration into electrically neutral oxide. The order-of-magnitude agreement of this estimate with the activation energies for lithium transport in oxide glasses (0.8 eV, i.e. ca. 18 kcal/mol [17,29]) is encouraging, although should be considered suggestive rather than conclusive.

In an actual electrochromic device, the lithium cation located out of the oxide phase is in fact embedded in an electrolyte, and in that region there is an additional stabilisation of 1–2 eV (about 25–45 kcal/mol) due to electrolyte polarisation [30]. In effect, there is little energy

gain when lithium approaches the neutral oxide surface. The energy minimum at the surface may be deep enough to result in actual adsorption, but in order to penetrate into the crystallite the lithium cation has to cross the barrier; moreover, the energy of the inner minimum is much higher. In effect, massive spontaneous lithium penetration into neutral oxide is highly unlikely.

This situation changes when the oxide cage is negatively charged by electron injection from the cathode (i.e. for the electrically neutral model cluster—bottom curve of Fig. 4). There is additional stabilisation energy of the order of 60 kcal/mol, which offsets the effect of electrostatic stabilisation in the electrolyte and provides the driving force for lithium to approach the crystallite. The barrier at the surface is now lowered to about 13 kcal/mol, and the inner minimum is practically as deep as that at the surface (the difference of 2 kcal/mol is well within the accuracy of the method). This implies that in this case an adsorbed ion has a good chance to migrate into the bulk.

The top curve of Fig. 4 corresponds to the situation where the model cluster (oxide cage $+Li^+$) carries a double positive charge, i.e. the oxide cage has a net positive charge (+1). The energy of the inner minimum is now 15 kcal/mol higher than that of the surface minimum, i.e. it is energetically even less favourable than for the electrically neutral oxide (middle profile); also the barrier is higher (18 kcal/mol). The entire profile is shifted to higher energies by another 50 kcal/mol. Explicit inclusion of the electrolyte polarisation energy, stabilising the lithium cation located at some distance from the cage, would readily offset the marginal lithium stabilisation in the oxide phase. This shows that at reversed electrode bias lithium would be driven out of the oxide, which is referred to as de-intercalation and is experimentally observed [3,5,6].

Inspection of the spin density distribution indicates that the spin density connected with the injected electron is accumulated mostly in the inner-layer; in consequence the tungsten ions in this layer bear slightly more electron density than those in the outer-layer do. The lithium cation is apparently drawn in the direction of the maximum electron density to get some share of it; hence the minimum of its energy is located close to the tungsten ions, although, owing probably to steric repulsion, not exactly within the corresponding layer of the cluster.

This interpretation is corroborated by analysis of charge redistribution within the system, accompanying lithium insertion into the oxide cluster. Fig. 6 shows the dependence of lithium charge upon lithium penetration into the bulk of the cluster for the W12 model (gauged by the reaction co-ordinate defined above). As already stated, the charge on lithium at large separation from the oxide cage approaches +1 for any charge state of the cluster. When the cation approaches the cage, its positive charge decreases and assumes the minimal value (about +0.2) at the cluster surface. This may be interpreted in terms of increasing covalency and charge transfer to lithium. Inside the cluster

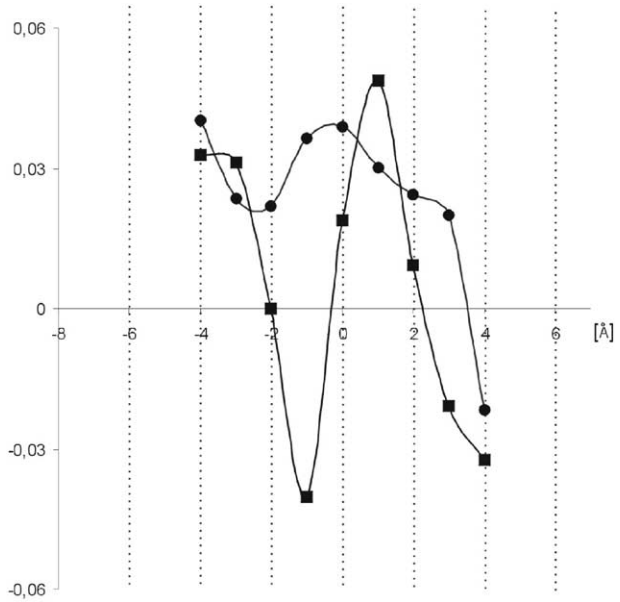

Fig. 7. Changes of the charges on all (symmetry equivalent) tungsten atoms of the outer (squares) and of the inner (circles) layer of the $[W_{12}O_{52}H_{36}]^{-1}$ cluster.

the positive charge on lithium slightly increases in the vicinity of the energy barrier, to decrease again at the energy minimum.

Evidently, the electrons acquired by lithium are effectively drawn from the surrounding tungsten atoms; with the oxygens mediating charge transfer. This follows from Fig. 7, displaying the corresponding changes of the charges on all the (symmetry equivalent) tungsten atoms of the outer (squares) and of the inner (circles) layer of the oxide cage with an injected extra electron, which is located predominantly on tungsten d orbitals. The charges in the lithium-free cluster are taken as reference.

Upon lithium approach, the (positive) charge on the tungstens of the inner-layer registers an almost monotonic increase—with the exception of an insignificant minimum, roughly coinciding with the position of the inner minimum in the energy profile. It seems that at this point Li^+ might already be close enough to these tungsten atoms to use the excess electrons for extra binding. By and large, the effect is neither large nor spectacular. In contrast, charge redistribution in the outer tungsten layer (through which lithium is inserted into the crystallite) undergoes much more dramatic and more diversified changes. Evidently, the tungsten atoms in this layer effectively donate electrons to the lithium ion when it approaches the surface and acquire some electron density when lithium is at the position of the energy barrier.

Lithium in the oxide phase retains some of its original charge, so it is justified to refer to it as a ‘cation’, in agreement with the accepted qualitative picture. Yet it should be noted in passing that this description is only approximate: as demonstrated above, in reality the lithium charge is fractional, since the cation gets dressed in electrons of the surrounding oxide matrix.

4. Discussion

Careful inspection of the energy profiles for W12 model suggests the following interpretation. In all charge states the lithium cation becomes stabilised at the cluster surface by both electrostatic and covalent interactions. The covalent part of this stabilisation seems to be similar in all cases, the electrostatic component, however, plays a decisively different role for various charge states. For the neutral system, which may be regarded as a crude model for Li^+ insertion into the oxide film with an injected extra electron, these effects add, which results in very high (by almost −130 kcal/mol) stabilisation of lithium at the oxide surface. In the case of the system with single positive charge (neutral cage) the long-range electrostatic interaction is absent and the overall lithium stabilisation at the surface amounts to −77 kcal/mol. For the $Li^+/[W_{12}O_{52}H_{36}]^{+1}$ system the long-range electrostatic interaction is repulsive and effective stabilisation of lithium at the surface is small, amounting to −23 kcal/mol.

In order to penetrate into the cluster interior, in all studied cases the lithium ion has to cross the energy barrier. While the stabilising effect at the surface seems to be connected with the presence of both oxygen and tungsten atoms in the outer-layer, the barrier occurring just below the surface seems to be due to the presence of the more distant pure-oxygen layer. The bonds with oxygens, of partly covalent character, are now broken, which decreases charge transfer and increases the positive charge on lithium. The barrier height is moderate for the neutral W12 model (about 12 kcal/mol) and systematically increases for charged models, up to 18 kcal/mol for the double positive charge on the system. Only in the case of the neutral system (the oxide with an injected electron) the second energy minimum found inside the cluster close to the internal tungsten-containing layer is deep enough (−11 kcal/mol with respect to the barrier top, less than 2 kcal/mol above the first minimum) to effectively bind the lithium cation inside the cluster. The potential energy minima found for the charged systems are too shallow (12 and 15 kcal/mol above the minimum corresponding to the cation stabilised at the surface) to bind lithium. Based on these differences in the shape of the energy profiles one can speculate that after electron injection into the film the lithium cation is very strongly stabilised at the crystallite surface and may then easily penetrate inside, to become equally strongly stabilised in its interior.

The (technologically crucial) lithium balance between the oxide phase and the polymer electrolyte is governed by the interplay between the combined covalent and electrostatic Li^+ stabilisation in the oxide phase and the additional stabilisation of the lithium cation in polymer environment, due to electrolyte polarisation. The latter was estimated as ca. 25–45 kcal/mol, [30] which shifts the reference energy level down. A different methodology is necessary to treat this effect [31].

In view of the recent results [30,31] our calculations confirm that, even when the polarisation contribution is taken into account, lithium intercalated into the oxide covered by a polymer layer is substantially stabilised inside the cluster when an extra electron is injected into the film. For neutral films the stabilisation is predicted to be much smaller, comparable to that expected in the polymer, so that only a marginal amount of lithium is expected to penetrate into the oxide. In the case of reversed voltage bias the lithium cations in the oxide phase are strongly destabilised and should be swept out of the crystallite.

Some information may be also extracted with respect to lithium migration within the film. When the cluster is negatively charged, the energy barrier for leaving the cluster amounts to 11 kcal/mol, but it appears that lithium transport inside the cluster is almost barrierless.

These specific conclusions should be taken with some reservation. As a matter of fact, the three-layer model we are using (W12) is more realistic than the two-layer model; the latter has no ‘bulk’ in the proper sense. Nevertheless, one has to bear in mind that even in the W12 model the ‘bulk’ is represented only by a single inner-layer, which may be insufficient and potentially produce some artefacts. Unfortunately, it is not possible at the present stage to handle a larger cluster. Therefore, the present results have to be considered as a first step in the quantum chemical description of the intercalation process. We believe that the gross description of its energetics, crucial to understand the role of the polymer electrolyte, is correct, and so are the predicted general trends. The specific values of the obtained activation energies may be less accurate, and need to be investigated in more detail in the future.

Acknowledgements

The computing facilities were supported by a grant from the State Committee for Scientific Research (KBN/SGI_ORIGIN_2000/UJ/042/1999). This work was partly supported under the EU FP5 Project ELEVAG, reference ENK6-CT-2001-00547.

References

[1] C.G. Granqvist, Solar Energy Mater. Solar Cells 60 (2000) 201.
[2] K. Bange, Solar Energy Mater. Solar Cells 58 (1999) 1.
[3] S. Papaefthimiou, G. Leftheriotis, P. Yianoulis, Electrochim. Acta 46 (2001) 2145–2150.
[4] G. Leftheriotis, S. Papaefthimiou, P. Yianoulis, A. Siokou, Thin Solid Films 384 (2001) 298–306.
[5] S.K. Deb, Solar Energy Mater. Solar Cells 39 (1995) 191–201.
[6] S. Papaefthimiou, G. Leftheriotis, P. Yianoulis, Solid State Ionics 139 (2001) 135–144.
[7] S.H. Lee, M.J. Seong, H.M. Cheong, E. Ozkan, E.C. Tracy, S.K. Deb, Solid State Ionics 156 (2003) 447–452.
[8] M. Green, K. Pita, Solar Energy Mater. Solar Cells 43 (1996) 393–411.

[9] O.F. Schirmer, K.W. Blazey, W. Berlinger, R. Diehl, Phys. Rev. B 11 (1975) 4201.
[10] O.F. Schirmer, Z. Phys. B 24 (1976) 235.
[11] O.F. Schirmer, V. Wittwer, G. Baur, G. Brandt, J. Electrochem. Soc. 124 (1977) 749.
[12] C. Bechinger, M.S. Burdis, J.-G. Zhang, Solid State Commun. 10 (1997) 753–756.
[13] J.-G. Zhang, D.K. Benson, C.E. Tracy, S.K. Deb, A.W. Czanderna, C. Bechinger, J. Electrochem. Soc. 144 (1997) 202.
[14] A. Hjelm, C.G. Granquist, J.M. Wills, Phys. Rev. B 54 (1996) 2436.
[15] B. Vuillemin, O. Bohnke, Solid State Ionics 68 (1994) 257.
[16] J. Wang, J.M. Bell, I.L. Skryabin, Solar Energy Mater. Solar Cells 59 (1999) 167–183.
[17] S.H. Garofalini, J. Power Sources 110 (2002) 412–415.
[18] G.E. Brown, V.E. Henrich, W.H. Cosey, D.O. Clark, C. Eggleston, A. Felmy, M.A. Henderson, Appl. Catal. A 251 (2003) 143.
[19] G. Pacchioni, Surf. Rev. Lett. 7 (2000) 277.
[20] P. Persson, R. Bergstrom, L. Ojamae, S. Lunell, Adv. Quantum Chem. 41 (2002) 203.
[21] V.E. Henrich, P.A. Cox, Appl. Surf. Sci. 72 (1993) 277.
[22] R. Tokarz-Sobieraj, K. Hermann, M. Witko, A. Blume, G. Mestl, R. Schlogl, Surf. Sci. 489 (2001) 107–125.
[23] A. Haras, M. Witko, D.R. Salahub, K. Hermann, R. Tokarz, Surf. Sci. 491 (2001) 77–87.
[24] E. Broclawik, Adv. Quantum Chem. 33 (1999) 349–367.
[25] M. Najbar, E. Brocławik, A. Góra, J. Camra, A. Białas, A. Wesołucha-Birczyńska, Chem. Phys. Lett. 325 (2000) 330–339.
[26] E. Broclawik, A. Góra, M. Najbar, Comput. Chem. 24 (2000) 405–410.
[27] DMol, Insight II release 96.0, User Guide, Molecular Simulations, San Diego, 1996.
[28] P.R. Bueno, R.C. Faria, C.O. Avellanda, E.R. Leite, L.O.S. Bulhoes, Solid State Ionics 158 (2003) 415.
[29] L. Laby, L.C. Klein, J. Yan, M. Greenblatt, Solid State Ionics 81 (1995) 217.
[30] A. Eilmes, R.W. Munn, A. Góra, J. Chem. Phys. 119 (2003) 11467–11474.
[31] A. Eilmes, R.W. Munn, J. Chem. Phys. 120 (2004) 7779–7783.